



TECHNICAL ARTICLE

Tribological Studies and Optimization of Two-Body Abrasive Wear of NaOH-Treated *Vachellia Farnesiana* Fiber by Additive Ratio Assessment Method

Francis A. Albert, Daniel James D. Jafrey , G. Karthik Pandiyan, Immanuel W. John, S. Hariharan, A. Guna, L. Haribaskar, Kumar G. Sathish, and Chandran Mohanraj

Submitted: 20 January 2022 / Revised: 28 March 2022 / Accepted: 5 May 2022 / Published online: 29 June 2022

In the modern day, natural fiber-reinforced composites are becoming one of the most appealing materials for research. *Vachellia farnesiana* fibers were chosen for this study and extracted manually using a retting process. Chemically, the resulting fiber was treated with sodium hydroxide (NaOH) solutions and then crushed and reinforced in epoxy matrix. The hand layup procedure was used to create a composite containing 0, 3, 6 and 9% NaOH-treated *Vachellia farnesiana* (NVF). Two-body abrasive wear characteristics were studied for the manufactured NVF composites. Material, load (N) and sliding distance (m) were used as input factors, while coefficient of friction (COF) and specific wear rate (SWR) were analyzed as output features. ANOVA was used for evaluating the input characteristics over the output characteristics which revealed that applied load (42.70%) was the dominant factor for SWR and for COF material was the dominant factor (59.89%). The wear mechanisms were studied using worn surface morphology which revealed that the addition of fillers resulted in increased wear resistance. Finally, using the additive ratio assessment approach, the result was optimized. From the output of ARAS method, it was found that the 9 wt.% material, 20N load and 100 m sliding distance have better wear resistance.

Keywords ARAS, load, specific wear rate, *vachellia farnesiana*

1. Introduction

Because of its strong adherence when fillers are added, epoxy resin is one of the most extensively used polymer matrixes. Epoxy material is a better material because of its improved hardness, resistance to humidity, enhanced hardness characteristics and better thermal and mechanical qualities (Ref 1). Typically, fillers are added to the epoxy matrix to improve its properties. Several scholars have added fillers in the form of particles and short fibers in recent years (Ref 2). It is simple to manufacture and may be subjected to a variety of machining procedures. The characteristics of epoxy filled composites are determined by various factors, including the shape and size of the fillers, as well as any surface modification of the fillers. Wear, dimensional stability and heat dissipation are all attributes that surface-modified fillers can improve (Ref 3).

Francis A. Albert, Daniel James D. Jafrey, Immanuel W. John, S. Hariharan, A. Guna, and L. Haribaskar, Department of Mechanical Engineering, K.Ramakrishnan College of Engineering, Tiruchirappalli, India; **G. Karthik Pandiyan,** Department of Mechanical Engineering, Sri Vidya College of Engineering and Technology, Virudhunagar, TamilNadu, India; **Kumar G. Sathish,** Department of Mechanical Engineering, K.Ramakrishnan College of Technology, Tiruchirappalli, India; and **Chandran Mohanraj,** Department of Mechanical Engineering, M. Kumarasamy College of Engineering, Karur, India. Contact e-mail: jafrey.daniel@gmail.com.

In the past, several researchers have added metal fillers like silicon carbide, boron carbide and alumina to the epoxy matrix and reported improvements in properties (Ref 4, 5). Graphite and molybdenum sulfide-type lubricant fillers have been added to improve the tribological properties (Ref 6). Several varieties of fillers, including natural and synthetic fillers, are used to improve the wear resistance of epoxy composites. Many researchers have tried to improve this performance by adding various reinforcing agents and fillers, including a range of nanoparticles (Ref 7). In the present scenario, the epoxy material has been reinforced with natural fibers which possesses several advantages than synthetic fibers. These natural fibers can be extracted from various parts of the plant like bark, stem and root. To increase the properties of the natural fibers, it has been treated by several chemical treatments and the change in properties has been reported (Ref 8). Alkali-based treatment has been mostly carried out by several researchers. Alkali-based treatment is widely used when natural fibers are reinforced in epoxy matrix (Ref 9).

One of the most frequent material removal processes encountered in an industry is wear, of which the main contributor is abrasive wear. It can be defined as the removal of solid particles by the action of hard-type particles moving from another body. The movement of hard particles across a solid surface causes abrasive wear (Ref 10). The creation of grooves in the surface caused by the pressing of abrasive grit on the surface and the removal of material at the front end of the abrasive particles that are sliding on the surface are the two mechanisms that cause abrasive wear. The amount of material removed is proportional to the volume of the groove formed by the relative motion and is determined by the sliding distance. Atkins (Ref 11) came to the conclusion that the wear of any

Table 1 Chemical constituents of treated and untreated fibers (Ref 9)

Cellulose Fiber name	Diameter, μm	Density, kg/m^3	Cellulose, wt. %	Hemicellulose, wt. %	Lignin, wt. %	Wax, wt. %	Moisture Content, %	Ash, wt. %
Untreated <i>Vachellia farnesiana</i>	231 \pm 2.68	1270 \pm 4.48	38.3	12.1	9.2	3.4	11	6.21
NaOH-treated <i>Vachellia farnesiana</i>	183 \pm 3.65	1352 \pm 3.32	47.8	7.3	4.7	1.8	6.3	7.3

material is determined by properties such as modulus, toughness and strength.

Xing and Li (Ref 12) used nanoparticles in the 500 nm range, while Durand et al. (Ref 13) used nanoparticles in the 100 nm range, to investigate the influence of fillers in the epoxy matrix and study the composites' wear rate. Durand came to the conclusion that wear resistance increases as particle size increases, which contradicts Xing and Li's findings. Because of the differences in testing parameters, the results are contradictory. Durand applied a weight of 10 N, whereas Xing and Li applied a load of 2 N. Any material abrasive wear is determined by the contact surface pressure between the material and the counter surface. When pressure rises, many mechanisms emerge, including plowing, cutting and cracking. The abrasive particles plow into the matrix and reinforcement, creating a stress field. Compressive stress forms at the front end of the sample, while tensile stress forms behind the abrasive particles. The movement of material over the abrasive surface causes cracking at the matrix–reinforcement interface. The cutting mechanism is located at the matrix–reinforcement contact, and it is characterized by the creation of a transfer layer on the counter face (Ref 14).

Vachellia farnesiana was chosen as the fiber source in this study. *Vachellia farnesiana*, often known as needle bush, is a legume shrub or small tree native to India and Africa. In most places, it is evergreen. It grows to a height of up to 30 feet. Each leaf is accompanied by a pair of thorns in the branch at its base. To release the fiber bundles, the bark was first taken from the tree and submerged in water for 20 days. Manual retting was used to separate the fibers from the loosened bark (Ref 8). Finally, to remove moisture from the surface, the resulting fibers were dried in the sun for seven days. Chemically, the fiber was treated with 5 wt.% NaOH (Ref 9).

All stages of product and process development are included in Taguchi's optimization technique. The design of parameters is a critical component in achieving good quality and low cost. The Taguchi design of experiment is used to determine the ideal parameter levels. The percentage contribution of each input parameter to the output parameters is calculated using the ANOVA approach. Several authors have used the Taguchi methodology for designing the experiments and ANOVA for studying the input parameters over the output parameters (Ref 15). Optimization of process parameters is usually employed to find the optimized values among the solutions. One of the most important parts of decision theory is multi-attribute decision-making (MADM), and related research has risen in popularity in recent years. After it was discovered that information could be both quantitative and qualitative, and that different measurement units cause complications in specific MADM problems, the additive ratio assessment system (ARAS) approach was proposed (Ref 16). Karthik Pandiyan et al. (Ref 17)

optimized the wire electrical discharge machining of aluminum-based composites and optimized the output parameters by CODAS method. Similarly many research had been published by several researchers by optimizing the output. Sihombing (Ref 18) et al. utilized the ARAS method for selecting the location for opening an English coaching center. According to the findings of the study, the ARAS approach is an excellent tool for decision assistance when determining the best alternative location.

From the widespread literature survey, there are no works related to abrasive studies of epoxy/NVF composites. The ARAS method was widely used in decision-making processes, but it was never used to optimize the output parameters of any experiments. The composites were manufactured by hand using a layup process, and the samples were tested for mechanical, thermal and morphological characteristics. The abrasive wear experiments were designed according to the Taguchi design of experiments. The output of the experiments was optimized using the ARAS method.

2. Materials and Methods

The material selected, manufacturing method and the tribological testing details are discussed in the following section

2.1 Materials Selected

The schematic of the work is shown in Fig. 1. Epoxy with a grade name of LY 556 was selected as a matrix in the present investigation. The hardener selected in the present study was HY 951. Initially, the fibers were extracted from the barks. The extracted barks were processed into fibers by the process of manual retting. In our previous studies, the extracted VF fibers were treated under the three conditions (no treatment, NaOH-treated and Hcl-treated) and their properties were studied. From the output of the studies, it was found that the NaOH-treated fibers resulted in better enhancement in properties. The alkali-treated VF fibers was selected as a reinforcement in the present study. When the treatment is completed, it was washed with water which ensures that the traces of chemicals has been removed. The treated fibers were dried, and it was made into powder form which can be used as a reinforcement (Ref 9).

2.2 Manufacturing Method

Composites were manufactured using the hand layup method. Four different types of samples with (0, 3, 6 and 9 wt. %) designated as 1, 2, 3 and 4 were reinforced in the epoxy matrix. Initially, a mold release agent was applied to the mold to enable proper material removal from the surface. The ratio of

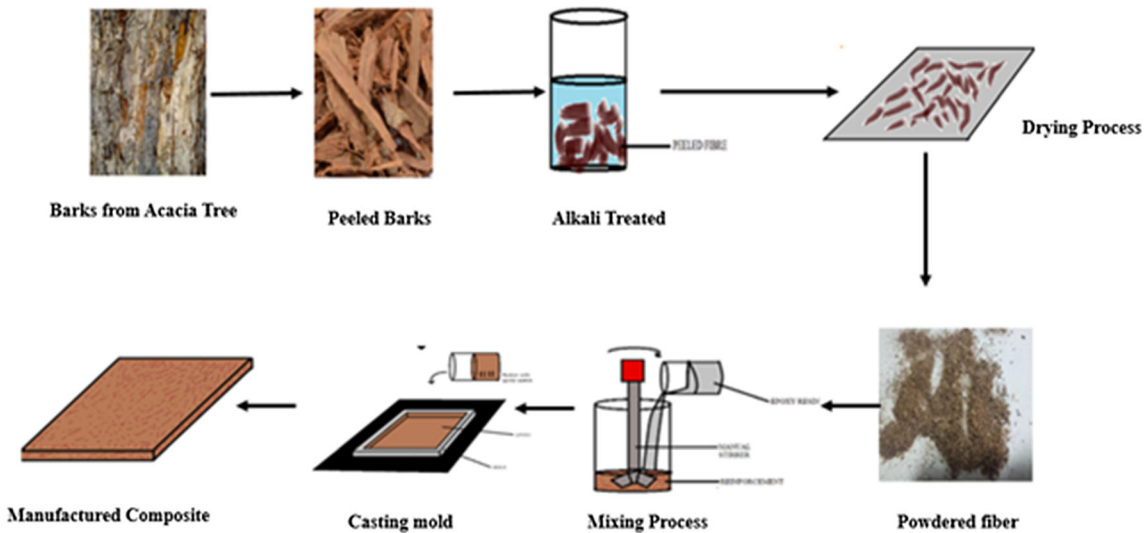


Fig. 1 Schematic diagram of manufacturing of composites

Table 2 Input parameter and their levels

Sl. No.	Parameters	Level 1	Level 2	Level 3	Level 4
1	Material, wt. %	0 (1)	3 (2)	6 (3)	9 (4)
2	Load, N	5	10	15	20
3	Sliding Distance, m	100	200	300	400

epoxy to hardener was kept at a 10:1 ratio. The reinforcement was added to the mixture of epoxy and hardener. The mixed solution was poured into the die material, and it was allowed to cure at room temperature. Once the curing is complete, the composites fabricated were taken out and the samples of wear test were cut according to the ASTM standards.

2.3 Abrasive Wear Studies

To determine friction and wear values, the tribological properties of polymer composite materials must be studied. Abrasive wear tests were done as per the ASTM standard (ASTM G99-05), utilizing a pin-on-disk setup to explore the tribological properties. A 320 grit size paper was pasted on the disk, which acted as an abrasive medium in the present investigation. The input parameters considered for the study are material (wt.%), load (N) and sliding distance (m). The process parameters and their level are shown in Table.2. Abrasive paper of 320 grit size was pasted on the disk which acted as a surface for sliding. The output parameters studied were COF and SWR, and their formulas are shown in Eq 1 and 2. A scanning electron microscope was used to examine the worn surface morphology of the abraded surfaces.

$$SWR = \frac{m_1 - m_2}{\rho XNS} \quad (\text{Eq 1})$$

where m_1 and m_2 are weight of specimen before and after test, ρ is the material density (g/mm^3), N is the applied load (N), and S is the sliding distance (m).

$$COF = \frac{\text{Frictional Force}(F)}{\text{Applied Load}(N)} \quad (\text{Eq 2})$$

3. Results and Discussion

The experiment was carried out according to L'16 orthogonal array, and the results are tabulated in Table 3.

3.1 Coefficient of Friction

The COF value with respect to the input parameters is represented in the Table 3, and the main effect plot of the same is shown in Fig. 2. With respect to different sliding distances and material combinations, it can be deduced from Fig. 2 that as the load increases, the COF values drop. The COF showed a different trend when the sliding distance is taken into effect. When considering the addition of fillers, the COF values fall as the amount of reinforcement increases. In the case of filled polymer composites, the COF depends upon the adhesion and abrasion mechanisms. Therefore, there is a decrease in trends in COF when the amount of filler is increased.

Figure 2 depicts the variation of COF with relation to sliding velocity. From the previous literature, it is evident that the composites have better stability to friction when compared to the pure material. The values of COF were minimum in the case of a 400 m sliding distance when compared to other sliding distances. COF values first increase up to 200 m and then fall as the sliding distance is increased. Researchers in the past have reported some fluctuations in the case of phenolic resin or bisamide resin. However, in the present study, the values of COF change when compared to the previous study as

Table 3 Input parameters with their output responses for all the experiments

Sl. No.	Input Parameters			Output Parameters	
	Material, wt.%	Load, N	Sliding distance, m	SWR, mm ³ /N-m	COF, μ
1	1	5	100	7.032	0.2533
2	1	10	200	6.71	0.2482
3	1	15	300	4.489	0.2295
4	1	20	400	2.95	0.20825
5	2	5	200	7.052	0.23885
6	2	10	100	6	0.2278
7	2	15	400	3.6	0.21335
8	2	20	300	2.725	0.21165
9	3	5	300	4.653	0.2091
10	3	10	400	4.1	0.20485
11	3	15	100	5.025	0.20315
12	3	20	200	3.85	0.2091
13	4	5	400	4.056	0.20655
14	4	10	300	3.08	0.2006
15	4	15	200	3.604	0.20485
16	4	20	100	3.411	0.19465

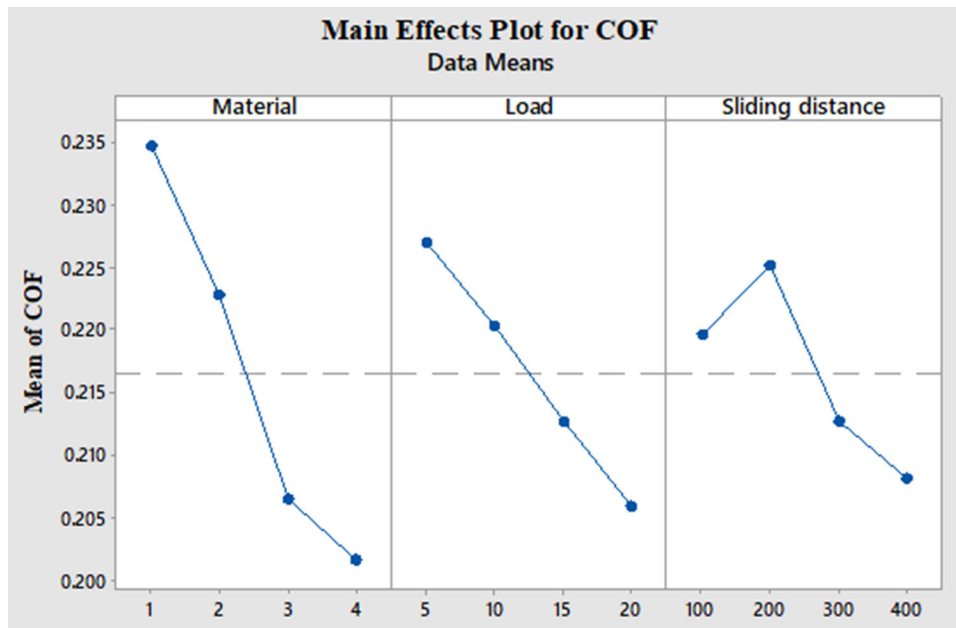


Fig. 2 Main effect plots for COF

the matrix and filler are entirely different. The fillers are exposed at the interface due to the matrix material's thermal softening, as the sliding distance increases. Due to the thermal softening, there is a separation of fillers from the matrix which acts as a third material resulting in fluctuation of COF values (Ref 19). In the case of polymer composites, the rolling effect of fillers under abrasive sliding circumstances led to decreased friction and wear, which is debatable (Ref 20). The added NVF fillers in the epoxy matrix, on the other hand, have a lower tendency to roll and are more likely to slide in the current investigation. As a result, when compared to the rolling friction, the sliding friction has a substantial impact, which is also evident from the worn surface morphology. Because of abrasion, the sliding friction lowers as the number of fillers increases, lowering COF values. Klaus (Ref 21) also reported

that there is an increase in wear resistance when the fillers content is increased in the epoxy matrix. In the case of epoxy/NVF composites, both adhesion and abrasion define the friction. From the figure, it can be seen that when the load is set at 40N there is a decrease in COF values. The reason for the decrease in COF values when the NVF is added at 9wt. % is the exposure of more amount of filler material, which acts as a barrier to wear, leading to a decrease in COF values.

3.2 Specific Wear Rate

Figure 3 shows the main effect plots of SWR rate with respect to load, sliding distance and material. From Fig. 3 it is evident that pure epoxy material showed highest rate of wear when compared to material combinations. The absence of filler

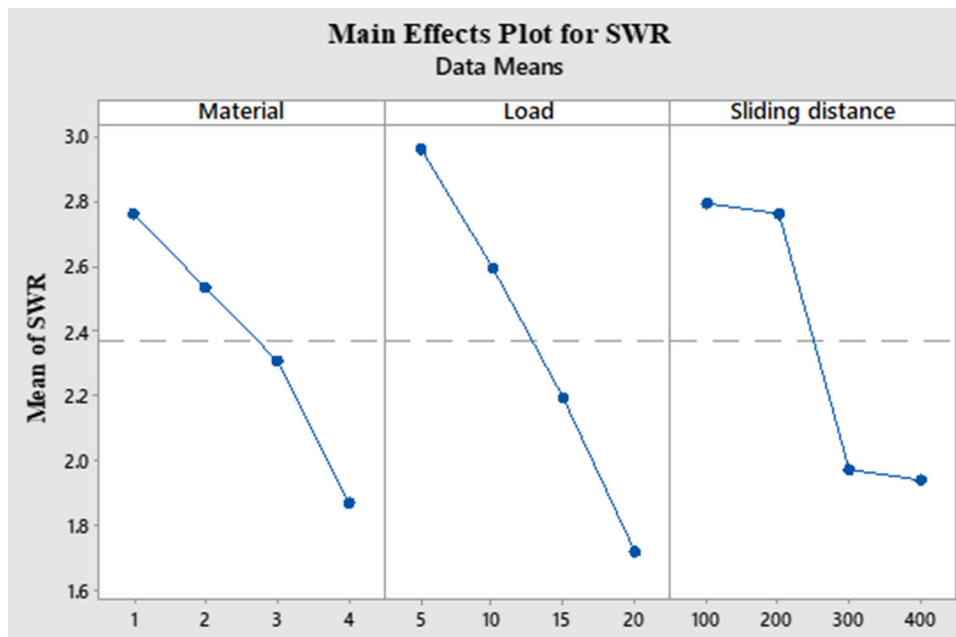


Fig. 3 Main effect plots of SWR

in the epoxy matrix led to increase in wear rate. Similar kind of trend in the case of pure materials without fillers was also observed by Narmadadevi et al. (Ref 1). When the amount of filler in the matrix is increased in epoxy/NVF composites, the wear rate is reduced. Thus, it can be clearly evident that the addition of NVF fillers to the epoxy matrix enhanced the wear resistance. Thus, the maximum wear resistance was found to be at 9 wt.% of material. As previously stated, the epoxy composites had a greater COF due to the fillers resistance to cutting. Frictional heating increased the temperature at the pin and disk interface. Composites could retain better mechanical strength under high temperatures because fillers have a stronger heat resistance. As a result, unlike pure epoxy, materials were not easily peeled off, resulting in lower wear rates for epoxy composites. Thus, it can be concluded that the addition of fillers had resulted in increase in wear resistance and vice versa in the case of pure epoxy composites (Ref 22)

When load and sliding distance are increased, the values of SWR decreased irrespective of all material. As in the case of COF, the filler material gets detached from the surface by the mechanism of plastic deformation under the conditions of increased load and sliding distance. According to Ozturk et al. (Ref 23), increasing the sliding speed accelerates the rate of impact loading induced by strong asperities on the counterface. On the abrasive surface, the removed material creates a transfer layer. The formed transfer layer acts as a lubricating layer which prevents the further removal of material from the matrix surface (Ref 24). In the case of sample 4, the SWR values were not affected when there was an increase in load and sliding velocity. SWR values increased up to 200 m, as in the case of COF, and SWR values decreased as the sliding velocity increased. The formation of transfer layer was the main reason for the decrease in SWR values at 400 m sliding distance. The formation of transformation layer on the counterface depends upon the factors like sliding distance, load and speed. The formed transfer layer acted as a lubricating layer during the abrasive wear process hindered increased the wear resistance.

Bahadur (Ref 24) also concluded that the formation of transfer layer had resisted the formation of wear.

The prime reason for increase at 200 m is due to the rubbing action between the interfaces which increase the wear rate. This thermal softening of the matrix material exposes the fillers at the interface, and as the load and sliding velocity increases, the fillers separate from the matrix, and the filler material functions as a third material, leading to the friction coefficient to oscillate. This raises the frictional thrust, which generates localized vibration at the sliding surface, causing the matrix to fracture and debond of fillers. Similar kinds of results were also reported by Formisano et al. (Ref 7). They also concluded that the addition of fillers to the epoxy matrix has resulted in increased wear resistance.

3.3 ANOVA Studies

Through the link between the variables, the ANOVA is used to analyze the effect of the input parameters (material, sliding distance and load) on the output variables (COF and SWR). The ANOVA is used to quantify the abrasive wear parameters that have a statistical impact on the output. The COF and SWR were examined in this study, with the lower the better characteristics. ANOVA value of the COF and SWR is shown in Table 4 and 5. From Table 4 and 5 it can be inferred that all the parameters were influential factors as their F value calculated was more than F table value. From Table 4 it can be seen that material (59.89%) was the contributing factor followed by applied load and sliding distance. In the case of SWR, the influencing factor was applied load (42.70%) was the dominating factor followed by sliding distance and material.

3.4 Worn Surface Morphology

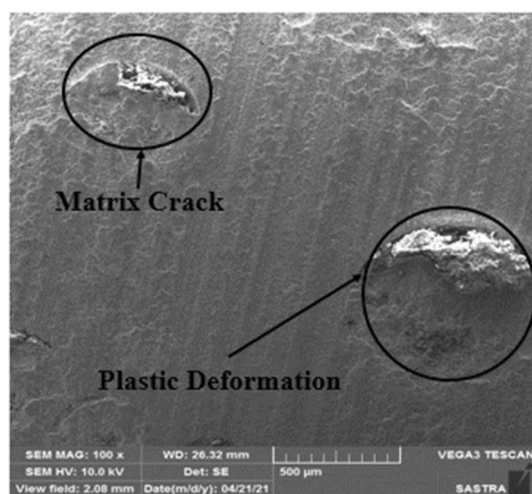
After sliding against the abrasive counterpart, key evidence on the wear mechanism is obtained on the worn surface of the specimens (Ref 25). The scanning electron microscope clearly shows the worn surface morphology of the abraded samples.

Table 4 ANOVA values of COF

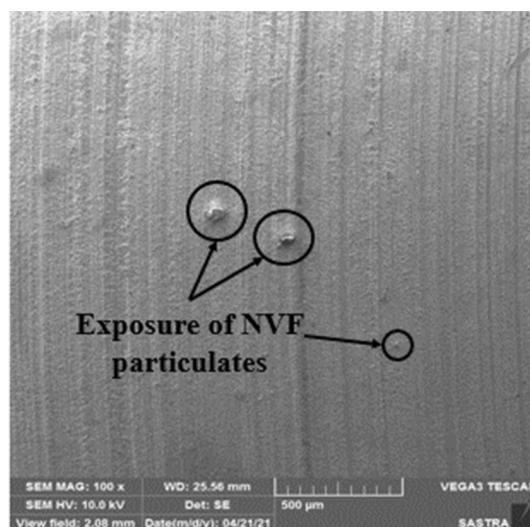
Source	DOF	Adj. SS	Adj. MS	F _{table}	F _{cal}	% contribution
Material, wt.%	3	0.002782	0.000927	4.76	30.40	59.89
Applied load, N	3	0.001002	0.000334	4.76	10.95	21.51
Sliding Distance, m	3	0.000677	0.000226	4.76	7.40	14.57
Error	6	0.000183	0.000031	4.03
Total	15	0.004645	100

Table 5 ANOVA values of SWR

Source	DOF	Adj. SS	Adj. MS	F _{table}	F _{cal}	% contribution
Material, wt.%	3	6.7349	2.2450	4.76	19.70	21.38
Applied load, N	3	13.4510	4.4837	4.76	39.35	42.70
Sliding Distance, m	3	10.6281	3.5427	4.76	31.09	33.74
Error	6	0.6837	0.1139	2.18
Total	15	31.4978	100

**Fig. 4** Worn surface morphology of sample 1

The sample 1 and 4 worn surface morphology is shown in Fig. 4 and 5. From Fig. 4, it is evident that the pure epoxy material has undergone severe damage under abrasive sliding conditions. The formation of matrix cracking perpendicular to the sliding direction and matrix deformation can be seen in the figure. The above-mentioned mechanisms were the prime reason for the greater amount of material loss. Similar kinds of results were also reported by Bassani et al. (Ref 26) In the case of Fig. 5, it can be concluded that the addition of fillers reduced the wear rate. In the case of sample 4, the exposure of fillers resulted in a decrease in wear rate, which can be seen in the worn surface morphology. The fillers act as third body particles, which reduces the wear rate. Thus, the experimental values correlated with the worn surface morphology studies.

**Fig. 5** Worn surface morphology of sample 4

4. Additive Ratio Assessment (ARAS) Method

The assignment of ranking to the choice alternatives is dealt with in multi-criteria decision-making situations. The utility function value is determined using the ARAS approach. Based on the output parameter and the weight criteria selected, the utility value determines the best feasible alternative or best optimal parameter.

Step 1: The creation of the decision matrix is the first step in the ARAS approach. The decision matrix, which is represented as follows, can be used to solve any discrete optimization problems on MCDM.

$$X = \begin{bmatrix} x_{01} & \text{amp}; x_{0j} & \text{amp}; \dots & \text{amp}; x_{0n} \\ x_{i1} & \text{amp}; x_{ij} & \text{amp}; \dots & \text{amp}; x_{in} \\ \vdots & \text{amp}; \vdots & \text{amp}; \vdots & \text{amp}; \vdots \\ x_{m1} & \text{amp}; x_{mj} & \text{amp}; \dots & \text{amp}; x_{mn} \end{bmatrix}, i = \overline{0, m}; j = \overline{1, n} \quad (\text{Eq 3})$$

$i=1, m, j=1, n$ M is the number of alternatives and n is the number of criteria

X_{ij} is the value representing the performance value of the i alternative in terms of the j criterion, and X_{0j} is the optimal value of j criterion.

If optimal value of j criterion is unknown, then

$$\begin{aligned} x_{0j} &= \text{imax}x_{ij}, \text{ if } \text{imax}x_{ij} \text{ is preferable;} \\ x_{0j} &= \text{imin}x_{ij}^*, \text{ if } \text{imin}x_{ij}^* \text{ is preferable.} \end{aligned} \quad (\text{Eq 4})$$

where x_{ij} are the performance values and the w_j are criteria weights.

Step 2: In the next stage we normalize the initial values for all the criteria by defining values \bar{x}_{ij} of normalized decision-making matrix \bar{X}

$$\bar{X} = \begin{bmatrix} \bar{x}_{01} & \dots & \bar{x}_{0j} & \dots & \bar{x}_{0n} \\ \vdots & \ddots & \vdots & \ddots & \vdots \\ \bar{x}_{i1} & \dots & \bar{x}_{ij} & \dots & \bar{x}_{in} \\ \vdots & \ddots & \vdots & \ddots & \vdots \\ \bar{x}_{m1} & \dots & \bar{x}_{mj} & \dots & \bar{x}_{mn} \end{bmatrix}; i = \overline{0, m}; j = \overline{1, n} \quad (\text{Eq 5})$$

The criteria with the highest desirable values (for positive beneficial traits) are normalized as follows:

$$\bar{x}_{ij} = \frac{x_{ij}}{\sum_{i=0}^m x_{ij}} \quad (\text{Eq 6})$$

Two levels of normalization are applied to the criterion with the lowest desirable values (for non-beneficial qualities).

$$x_{ij} = \frac{1}{x_{ij}^*}; \bar{x}_{ij} = \frac{x_{ij}}{\sum_{i=0}^m x_{ij}} \quad (\text{Eq 7})$$

Step 3: Normalized weighted matrix is carried out in third stage. In this stage the weight of each criteria is evaluated and it lies in the range of 0 to 1. The sum of weights w_j is equal to 1 and it is expressed in Eq 6. The normalized weighted matrix I is shown in Table 6.

$$\sum_{j=1}^n W_j = 1 \quad (\text{Eq 8})$$

$$\hat{X} = \begin{bmatrix} \hat{x}_{01} & \dots & \hat{x}_{0j} & \dots & \hat{x}_{0n} \\ \vdots & \ddots & \vdots & \ddots & \vdots \\ \hat{x}_{i1} & \dots & \hat{x}_{ij} & \dots & \hat{x}_{in} \\ \vdots & \ddots & \vdots & \ddots & \vdots \\ \hat{x}_{m1} & \dots & \hat{x}_{mj} & \dots & \hat{x}_{mn} \end{bmatrix}; i = \overline{0, m}; j = \overline{1, n} \quad (\text{Eq 9})$$

The normalized weights of all the criteria are expressed in the following equation.

$$\hat{x}_{ij} = \bar{x}_{ij} w_j; i = \overline{0, m} \quad (\text{Eq 10})$$

In Equation (10) the term w_j is the weight (importance) of the j criterion and \bar{x}_{ij} is j criterion normalized value.

Step 4: To determine the optimality function by

$$S_i = \sum_{j=1}^n \hat{x}_{ij}; i = \overline{0, m} \quad (\text{Eq 11})$$

where S_i is the value of optimality function of i^{th} alternative.

Table 6 Optimization of output values by ARAS method

Sl. No.	Input Parameters			Output		Normalized decision matrix		Weighted normalized matrix		Optimality Function	Utility Degree	Rank
	Material	Load	Sliding distance	SWR	COF	SWR	COF	SWR	COF	Si	Ki	
1	1	5	100	7.032	0.2533	0.001895	0.932732	0.0009	0.4664	0.4673	0.7669	16
2	1	10	200	6.71	0.2482	0.001985	0.951898	0.001	0.4759	0.4769	0.7827	15
3	1	15	300	4.489	0.2295	0.002968	1.02946	0.0015	0.5147	0.5162	0.8472	13
4	1	20	400	2.95	0.20825	0.004516	1.134507	0.0023	0.5673	0.5695	0.9346	7
5	2	5	200	7.052	0.23885	0.001889	0.989161	0.0009	0.4946	0.4955	0.8132	14
6	2	10	100	6	0.2278	0.00222	1.037142	0.0011	0.5186	0.5197	0.8529	12
7	2	15	400	3.6	0.21335	0.003701	1.107387	0.0019	0.5537	0.5555	0.9117	11
8	2	20	300	2.725	0.21165	0.004889	1.116282	0.0024	0.5581	0.5606	0.92	10
9	3	5	300	4.653	0.2091	0.002863	1.129895	0.0014	0.5649	0.5664	0.9295	9
10	3	10	400	4.1	0.20485	0.003249	1.153337	0.0016	0.5767	0.5783	0.9491	5
11	3	15	100	5.025	0.20315	0.002651	1.162988	0.0013	0.5815	0.5828	0.9565	3
12	3	20	200	3.85	0.2091	0.00346	1.129895	0.0017	0.5649	0.5667	0.93	8
13	4	5	400	4.056	0.20655	0.003285	1.143844	0.0016	0.5719	0.5736	0.9413	6
14	4	10	300	3.08	0.2006	0.004325	1.177772	0.0022	0.5889	0.591	0.97	2
15	4	15	200	3.604	0.20485	0.003697	1.153337	0.0018	0.5767	0.5785	0.9494	4
16	4	20	100	3.411	0.19465	0.003906	1.213774	0.002	0.6069	0.6088	0.9992	1

The values of calculated S_i shown in Table 6. The higher value of S_i considered as best value and the lower value is considered as worst.

The optimality function S_i has a direct and proportional relationship with the weights w_j of criteria and values x_{ij} and. When the value of S_i is in the higher side, it is most effective. The priorities were given as per S_i value and to evaluate and rank the decision alternatives. The degree of utility is determined by the ratio of S_i value to the S_o value. The S_o is the sum of all the weighted decision matrix value for the ideal best value. The utility degree K_i of an alternative a_i is calculated as per Eq 12, and the same is shown in Table 6.

$$K_i = \frac{S_i}{S_o} \quad (\text{Eq 12})$$

S_i and S_o are the optimality criterion values.

From the result, it is observed that estimated values of K_i values lie in between from 0 to 1.

According to the values of utility degree, the ranking of alternatives is $A16 < A14 < A11 < A15 < A10 < A13 < A04 < A12 < A09 < A08 < A07 < A06 < A03 < A05 < A02 < A01$. From Table 6 it can be seen that the experiment number 16 has the highest utility value and it is the best combination which gives the best output.

5. Conclusion

Composites made of epoxy/NVF were fabricated by hand layup process. The manufactured composites were evaluated for tribological characteristics by two-body abrasive wear tests. The output parameters were optimized by the ARAS method. The conclusion drawn from the present study is as follows:

- The fiber was initially treated with NaOH and was made into powder form for making the composites.
- The samples for two-body abrasive wear test were manufactured by the process of hand layup process.
- When COF is considered, it is a minimum at 40N load, 9wt. % material and a sliding distance of 400 m. The presence of reinforcement in the epoxy matrix which acted as a barrier was the prime reason for increase in abrasive wear resistance and decrease in COF values.
- In the case of SWR, the pure epoxy samples resulted in the greatest amount of weight loss due to the absence of reinforcement in it and the addition of fillers resulted in less wear loss.
- The formation of a transfer layer on the counterface at a higher sliding distance was the main reason for the lower amount of COF and SWR.
- The worn surface morphology of the abraded samples revealed that the presence of NVF had resulted in reduction of wear grooves matching the experimental studies. The absence of the fillers in A1 samples resulted in more damage.
- The optimization by the ARAS method revealed that experiment number 16 has the highest utility value of 0.992, making it the best one.
- This work can be extended by treating the fibers with different chemical treatments and reinforcing them in an epoxy matrix and studying their properties.

- The accuracy of the results is restricted to the limited number of experiments due to the limited number of process parameters. Hence, more experiments can be done for selection of process which can give a wide range of results. Thus, the ARAS method can be extended for several other applications.

References

1. N. Narmadadevi, V. Velmurugan, R. Prabhakaran, and R. Venkatakrishnan, Effect of Filler Content on the Performance of Epoxy/Haritaki Powder Composite, *Lect. Notes Mech. Eng.*, 2022, **2014**, p 277–283
2. D.J. Daniel and K. Panneerselvam, Processing of Polypropylene/Spheri Glass 3000 Nanocomposites by Melt Intercalation Method, *Procedia Technol.*, 2016, **25**, p 1114–1121. <https://doi.org/10.1016/j.protcy.2016.08.225>
3. Y. Kang, X. Chen, S. Song, L. Yu, and P. Zhang, Friction and Wear Behavior of Nanosilica-Filled Epoxy Resin Composite Coatings, *Appl. Surf. Sci.*, 2012, **258**(17), p 6384–6390. <https://doi.org/10.1016/j.apsusc.2012.03.046>
4. M.S. Bhagyashekar and R.M.V.G.K. Rao, Effects of Material and Test Parameters on the Wear Behavior of Particulate Filled Composites Part 2: Cu-Epoxy and Al-Epoxy Composites, *J. Reinf. Plast. Compos.*, 2007, **26**(17), p 1769–1780
5. G. Shi, M.Q. Zhang, M.Z. Rong, B. Wetzel, and K. Friedrich, Sliding Wear Behavior of Epoxy Containing Nano-Al₂O₃ Particles with Different Pretreatments, *Wear*, 2004, **256**(11–12), p 1072–1081
6. X. Li, Y. Gao, J. Xing, Y. Wang, and L. Fang, Wear Reduction Mechanism of Graphite and MoS₂ in Epoxy Composites, *Wear*, 2004, **257**(3–4), p 279–283
7. A. Formisano, L. Boccarusso, FC. Minutolo, L. Carrino, M. Durante, and A. Langella, 2016, Wear Behaviour of Epoxy Resin Filled with Hard Powders, *AIP Conf. Proc.*, p. **1769**
8. R. Vijay, J.D. James Dhillip, S. Gowtham, S. Harikrishnan, B. Chandru, M. Amamath, and A. Khan, Characterization of Natural Cellulose Fiber from the Barks of Vachellia Farnesiana, *J. Nat. Fibers*, 2020 <https://doi.org/10.1080/15440478.2020.1764457>
9. V. Raghunathan, J.D.J. Dhillip, G. Subramanian, H. Narasimhan, C. Baskar, A. Murugesan, A. Khan, and A. Al Otaibi, Influence of Chemical Treatment on the Physico-Mechanical Characteristics of Natural Fibers Extracted from the Barks of Vachellia Farnesiana, *J. Nat. Fibers*, 2021 <https://doi.org/10.1080/15440478.2021.1875353>
10. D.J. Daniel and K. Panneerselvam, Investigation on Thermal and Tribological Properties of Polypropylene / Spheri Glass 3000 Composites Processed by Melt Intercalation Method, *SILICON*, 2019, **11**(6), p 2885–2894
11. A.G. Atkins, Toughness in Wear and Grinding, *Wear*, 1980, **61**(1), p 183–190
12. X.S. Xing and R.K.Y. Li, Wear Behavior of Epoxy Matrix Composites Filled with Uniform Sized Sub-Micron Spherical Silica Particles, *Wear*, 2004, **256**(1–2), p 21–26
13. J.M. Durand, M. Vardavoulas, and M. Jeandin, Role of Reinforcing Ceramic Particles in the Wear Behaviour of Polymer-Based Model Composites, *Wear*, 1995, **181–183**, p 833–839
14. G.Y. Lee, C.K.H. Dharan, and R.O. Ritchie, A Physically-Based Abrasive Wear Model for Composite Materials, *Wear*, 2002, **252**(3–4), p 322–331
15. K.P. Jafrey and D. Daniel, Study on Tensile Strength, Impact Strength and Analytical Model for Heat Generation in Friction Vibration Joining of Polymeric Nanocomposite Joints, *Polym. Eng. Sci.*, 2017, **57**(5), p 495–504. <https://doi.org/10.1002/pen.24443>
16. N. Liu and Z. Xu, An Overview of ARAS Method: Theory Development, Application Extension, and Future Challenge, *Int. J. Intell. Syst.*, 2021, **36**(7), p 3524–3565
17. G. Karthik Pandiyan, T. Prabaharan, D. Jafrey Daniel James, and V. Sivalingam, Machinability Analysis and Optimization of Electrical Discharge Machining in AA6061-T6/15wt % SiC Composite by the Multi-Criteria Decision-Making Approach, *J. Mater. Eng. Perform.*, 2022, **31**(5), p 3741–3752. <https://doi.org/10.1007/s11665-021-06511-8>

18. V. Sihombing, Z. Nasution, M.A. Al Ihsan, M. Siregar, I.R. Munthe, V.M. Mulia Siregar, I. Fatmawati, and D.A. Asfar, Additive Ratio Assessment (ARAS) Method for Selecting English Course Branch Locations, *J. Phys. Conf. Ser.*, 2021, **1933**(1), p 1–6
19. W. Österle, I. Dörfel, C. Prietzel, H. Rooch, A. Cristol-bulthé, G. Degallaix, and Y. Desplanques, A Comprehensive Microscopic Study of Third Body Formation at the Interface between a Brake Pad and Brake Disc during the Final Stage of a Pin-on-Disc Test, *Wear*, 2009, **267**, p 781–788
20. RN. Rothern, 2003 Particulate-Filled Polymer Composites Second Edition, *Technology*, (August), p 544, https://books.google.com/books/about/Particulate_filled_Polymer_Composites.html?id=4zFY5Yju3TQC. Accessed 17 January 2022
21. K. Friedrich, S. Fakirov, and Z. Zhang, 2005 Polymer Composites: From Nano-to-Macro-Scale, Springer, p 367
22. X. Hu and T. Lu, Inorganic Whiskers Reinforced Bismaleimide Composites, *J. Mater. Sci.*, 2005, **40**(7), p 1743–1748
23. B. Öztürk, F. Arslan, and S. Öztürk, Hot Wear Properties of Ceramic and Basalt Fiber Reinforced Hybrid Friction Materials, *Tribol. Int.*, 2007, **40**(1), p 37–48
24. S. Bahadur, The Development of Transfer Layers and Their Role in Polymer Tribology, *Wear*, 2000, **245**(1–2), p 92–99
25. C.A. Chairman, B. Thirumaran, S.P.K. Babu, and M. Ravichandran, Two-Body Abrasive Wear Behavior of Woven Basalt Fabric Reinforced Epoxy and Polyester Composites, *Mater. Res. Express*, 2020, **7**(3), p 035307
26. R. Bassani, G. Levita, M. Meozzi, and G. Palla, Friction and Wear of Epoxy Resin on Inox Steel: Remarks on the Influence of Velocity Load and Induced Thermal State, *Wear*, 2001, **247**(2), p 125–132

Publisher's Note Springer Nature remains neutral with regard to jurisdictional claims in published maps and institutional affiliations.